Wind fields and turbulence statistics in an urban street canyon

I. Eliasson[a],[*], B. Offerle[a], C.S.B. Grimmond[b], S. Lindqvist[a]

[a]*Urban Climate Group, Physical Geography, Göteborg University, SE 405 30 Göteborg, Sweden*
[b]*Department of Geography, Indiana University, Indiana, USA*

Abstract

This is the first paper of a long-term measurement campaign to explore wind, temperature, radiation and energy fields within an urban canyon. A canyon and a rooftop mast were installed in a canyon with an aspect ratio (Height/Width) of ~2.1 in Göteborg, Sweden. A number of instruments including sonic anemometers, radiometers and thermocouples were mounted in vertical profiles and across the width of the canyon. The experimental set-up, the characteristics of the canyon flow pattern and mean and turbulence statistics with respect to above canyon flow are examined using data collected under clear-sky conditions in summer and autumn 2003. Results show that under cross-canyon (within $60°$ of orthogonal) flow, a single helical vortex exists. High temporal resolution analysis suggests that eddies frequently penetrate the shear stress layer at the canyon top disrupting established flow patterns. A combination of complex building roof shapes and local topography may contribute to this effect by maintaining a high degree of turbulence. The profile of mean wind speed within the canyon and the relation with that above canyon depends on the ambient flow direction in relation to the canyon long axis. Turbulence statistics show results similar to other field studies, with turbulence kinetic energy and vertical mixing greatest toward the windward wall.
© 2005 Elsevier Ltd. All rights reserved.

Keywords: Urban canyon flow; Turbulence; Vortex

1. Introduction

The street canyon, a road and its flanking buildings, forms the basic geometric unit of the built environment. The geometry and materials that make up the canyons of a city greatly influence the urban climate (Arnfield, 1982; Oke, 1988). Knowledge of the processes of urban canyons is of great importance, both for understanding the micro-scale climate within the canyon, as well as for understanding the overall urban climate, for example, the coupling between the urban canopy and boundary layers. Within canyon processes are relevant to environ-

mental issues such as energy consumption, ventilation in buildings, dispersion of air pollutants (Vardoulakis et al., 2003), as well as human comfort and safety.

Wind and temperature fields, radiation and energy exchanges, and concentrations of air pollutants in urban street canyons are all topics that have been investigated through field experiments, scaled physical models in wind tunnels, and numerical modelling (Table 1). Most research has been focused on the complex flow patterns around buildings and within canyons as it is critical for the dispersion of windborne pollutants in the urban environment. This research is also important for understanding the relative significance of turbulent diffusion and canyon circulation in transferring entities, such as turbulent sensible heat and pollutants, through the roof-level plane.

*Corresponding author. Tel.: 46 31 773 2832;
fax: +46 31 773 1986.

E-mail address: ingegard@gvc.gu.se (I. Eliasson).

Table 1
Examples of full-scale, reduced scale and real world field observations of wind and turbulence in urban canyons, ordered by increasing Height/Width (H/W) ratio

Location	H/W	Roughness	Meas. period	Statistics	Vortex	Instruments	Author
MUST, DPG Utah	Low	$\lambda_P = 0.12$ Isolated roughness	Sept. 2001	TKE, U/U_H		so	Zajic et al. (2003)
Sydney	0.4	2 parallel rows of storage units, farmlands	Sept. 1993	Across & vertical	s		Johnson & Hunter (1999)
Salt Lake City	0.5^a	CBD	Oct. 2000			so	Allwine et al. (2002)
Reading	0.7	2 long barns, trees, grass in flat terrain	Sep.–Oct. 1996	W_{zh}/u^*, U/u^*, τ/τ_{RSL}	s	so, pa	Louka et al. (2000)
Cologne, Germany	1	4 lane road[T]	Aug.–Oct. 1997 Mar.–Apr. 1980 May 1981	$\sigma_{u,v,w}$ ws, $\sigma_{u,v,w}$	s	uvw	Yamartino & Wiegand (1986)
San Jose, California	1	CBD	Nov.–Dec. 1970	ws, wd	S	CO, uvw	Johnson et al. (1973) Dabbert et al. (1973)
Cardington, UK	1	Flat terrain	Oct. 90	u^*/U, $\sigma_{v,w}/U$, $\sigma_{v,w}/u^*$ u_z/u_{top} Stability, along/ across	h	so, pa	Davidson et al. (1995)
Basel	1	CBD	Nov. 2001–Jul. 2002	u_{*loc}/u_z, TKE/0.5 M^2, u_{*loc}/u_z, σ_w/u_{*loc}, S_w (vertical skewness)	s	so	Christen et al. (2002) Christen et al. (2003)
Zurich	1.2	$H = 20^a$, $H/W = 1$	131 turb. 18 months	$u/u(h)$, $\sigma_{u,t,w}/u_{*r}$ TKE (stability classes)	s	so	Rotach (1995)
Chicago	1.4	Canyon[T]	18 releases in 3 days	u,w	s,d	hb, hwa	DePaul & Sheih (1986)
Nantes, France	1.4	Dense urban	Jun.–Jul. 1999	Balloon residence time	s,d	so, pa, hb (CO profiles)	Vachon et al. (1999) Louka et al. (2002)
Copenhagen	1.4	Canyon[T]	185 days	Ambient wind versus U_w/U_0, σ_w		so	Nielsen (2000)
St. Louis, Missouri	1.5, 2	CBD	Aug.–Oct. 1971	ws, wd	s	CO, uvw	Dabbert et al. (1973)
Columbus, Ohio	1.52	$\lambda_P = 0.19$	11 cases	w	s,d	wm, pa, so	Arnfield & Mills (1994)
Oklahoma City	2^a	CBD	Jul. 2003	ws, wd, w		so	Brown et al. (2004)
Athens	2.5	CBD	Jul. 1997	W, U	s,d	pa, ca, T, IR	Santamouris et al. (1999)

Roughness characteristics within the vicinity of the site [plan area index, λ_P]. Statistics reported [ws = wind speed, wd = wind direction, w = vertical, u = horizontal, v = lateral]. Vortices observed [s = single, d = double, t = triple h = horse shoe]. Instrumentation used [so = sonic, wm = wind monitor, pa = propeller anemometer, hb = helium balloons, hwa = hot-wire anemometer, cu = cup anemometer, uvw = U, V, W components measured but other details not provided, T = Thermistors , IR–IR laser beam].

[a] Average T Typical of surroundings.

While numerous wind tunnel experiments and numerical modelling studies of urban canyon processes have been conducted, and these can be used to demonstrate critical features of canyon processes, relatively few full-scale real world studies exist (Table 1). Most of these field studies have focused on canyons with an aspect ratio (Height/Width ratio) around or above one where the ambient flow is perpendicular to the canyon long-axis, in order to describe the vortex circulation that appears. A helical vortex has been observed or inferred in field investigations (Johnson et al., 1973; Dabbert et al., 1973; DePaul and Sheih, 1986; Yamartino and Wiegand, 1986; Arnfield and Mills, 1994; Johnson and Hunter, 1999; Santamouris et al., 1999), predicted from numerical models (Sini et al., 1996; Baik and Kim, 1999; Kovar-Panskus et al., 2002) and wind tunnel or fluid channel studies (Baik et al., 2000; Kim and Baik, 2001; Kovar-Panskus et al., 2002). The formation of a secondary flow in the lower region of the canyon was observed in field studies by DePaul and Sheih (1986) and Arnfield and Mills (1994). Counter rotating vortices also appear in water channel studies and numerical simulations (e.g. Baik et al., 2000; Baik and Kim, 2002) for aspect ratios >2. Questions, however, remain about the conditions necessary for vortex (vortices) development and the controlling factors for the vortex (vortices) strength (Brown et al., 2000).

Field studies of comprehensive turbulence statistics are rare and most of them focus on the height variation in one profile (e.g. Nielsen, 2000; Christen et al., 2003). Measurements in the cross-section (upwind, centre, downwind) in combination with vertical variation (street level to above twice the height of the canyon, H) are of interest to numerical model evaluations and development. Some wind tunnel studies (e.g. Brown et al., 2000; Kastner-Klein and Rotach, 2004) and fluid channel experiments (Baik and Kim, 2002) have considered this but for practical reasons very few full-scale experiments have investigated the spatial patterns within the domain (e.g. Rotach, 1995; Brown et al., 2004). With a few exceptions (e.g. Rafailidis, 1997; Kastner-Klein and Rotach, 2004) scale model data typically have been gathered from simplified forms which do not have the complications of real world.

The scarcity of data on air flows around buildings and the fact that field experiments often lack knowledge of the upstream boundary conditions makes them difficult to use for rigorous computational fluid dynamics (CFD) model validation (Brown et al., 2000). Existing field data are used repeatedly and the literature reveals a need for field studies that: (1) investigate the vortex circulation in deep canyons (i.e. number of vortices) when the ambient flow is perpendicular and parallel to the canyon long-axis; (2) assess the turbulence structure within an urban canyon and its dependence on canyon geometry, ambient wind flow and above-canyon stability; (3) provide good documentation for the upstream boundary conditions; and (4) include simultaneous measurements of all components of the energy balance. With this in mind, the canyon and rooftop were instrumented in a street canyon ($H/W = 2.1$) in the city centre of Göteborg, Sweden. Not all of these weaknesses in the current literature can be treated with equal thoroughness. Here, the first two are given greater consideration.

2. Study site

Göteborg (57°42′ N, 11°58′E) is Sweden's second largest city with a population of approximately 500 000. The city, founded in 1621, has a classical European inner city structure. The study canyon is located in the oldest part of the city on the south side of the Göta river (Fig. 1a). The average aspect ratio in this area is around 2. The sky-view factor (SVF) ranges between 0.2 for streets perpendicular to the study canyon, and 0.7 for the main north–south street (Fig. 1b).

The study canyon (50 m long) is formed by adjacent, nearly symmetric buildings approximately 16 m high (H) (17 m for peak heights) decreasing to 13 m at the wall tops due to the slope of the roofs (Fig. 2). Because of the complex roof shape a precise canyon depth is difficult to define, but was taken to be 15 m, which is the approximate level where the roof pitch changes from steep to flat (Fig. 2). The width (W) of the street is 7.1 m, giving an aspect ratio of 2.1. The SVF of the street, determined from digital fisheye photographs (Grimmond et al., 2001) and a digital elevation model (DEM), is approximately 0.25. The street is oriented approximately N–S (340°) and is part of a 300 m long main street canyon consisting of 5 blocks that runs from an open square in the south towards the river. The façades of the buildings in the canyon are brick with windows covering approximately 25% of the wall surface. Vehicular traffic is light and is more frequently used by pedestrians. The street elevation is 2.54 m at the north intersection and 2.89 m at the south intersection. The mean aerodynamic characteristics based on morphometric analysis around the site are given in Table 2.

3. Methods

The instrumentation consists of ultrasonic anemometers (RM Young 81000) ('sonics') for measurements of three-dimensional wind velocities and turbulence, thermocouples (TCs) for measurements of air and surface temperature, and net radiometers for measurements of short- and long-wave radiation (Fig. 2). The instrumentation was installed beginning in January 2003, although complete data collection did not commence until the installation of the uppermost sonic
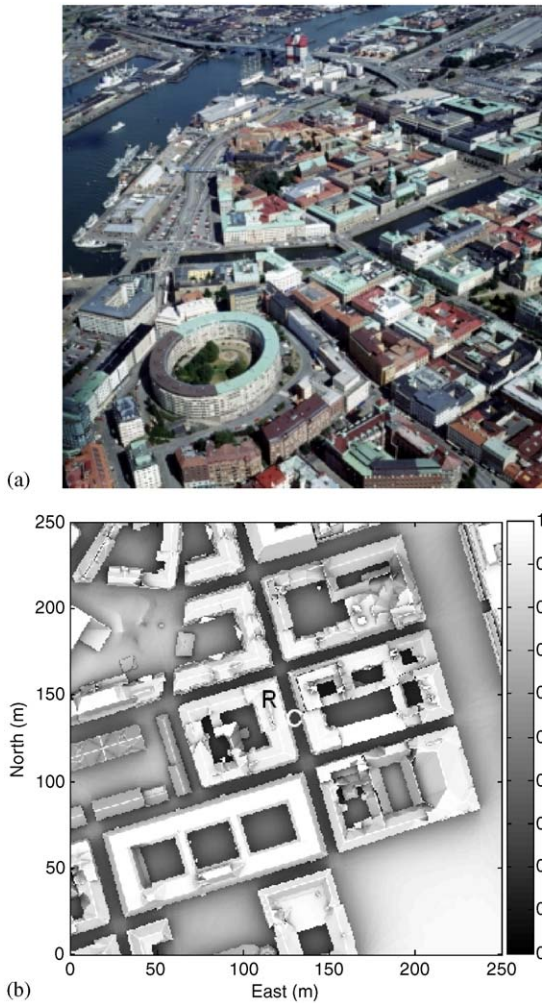
Fig. 1. (a) Oblique aerial photo of central Göteborg looking northeast. (b) Sky view factor (SVF) image of canyon area (calculated at surface height). C and R mark the locations of the canyon and roof mast.

Fig. 2. The canyon layout and instrumentation. Dimensions (m).

in June 2003. Surface wetness sensors and temperature and heat flux measurements for the road were added at later dates in 2003. Data collection ended in August 2004.

3.1. Instrumentation

The instruments are mounted on two masts, one located within the canyon and the other mounted on the roof of the western building (Figs. 2 and 3). The canyon mast consists of a 15 m high triangular lattice tower (0.4 m on a side) that is mounted at the block midpoint, 2 m from the eastern wall, and three horizontal booms, fastened to the vertical mast and the western wall (Fig. 3). A local traffic-agency rule (free space for cars up to 4.5 m height) imposed limitations on the placement of the lowest boom. Shorter booms extend northeast 0.7 m from the mast, immediately above the three main horizontal booms and at 3.1 and 14 m to give five vertical levels on the eastern side. In the canyon, three sonics are located at each of the main vertical levels providing a near regular grid of measurements. The east and west sonics are 1.4 m from the nearest wall and the middle sonics are slightly (0.2 m) to the east of canyon centre. TCs (Omega, T-type 36 AWG) for air temperature measurements are attached to each sonic approximately 0.1 m north and 0.2 m below the centre of the sampling volume of the sonic.

The roof mast, a triangular lattice, 0.4 m on a side at the base with tubular upper sections 0.033 m in diameter at the top, is mounted on the raised centre section of the building approximately 2 m higher than the canyon top (Fig. 2). Three sonics are mounted at 3 m (R1), 7 m (R2) and 14 m (R4) above the roof surface (Fig. 4). The lower sonics are mounted at the ends of booms extending

Table 2
Results of morphometric and log wind profile analysis for aerodynamic parameters by wind sector

Dir	Morphometric					Log wind profile			
	z_H	λ_p	λ_f	z_d	z_0	N	z_d	z_0	RMSE
0	16.8	0.58	0.43	10.7	2.1	356	7.3	1.6	0.12
30	16.8	0.51	0.51	11.1	2.2	539	9.6	1.8	0.12
60	20.4	0.62	0.39	12.8	2.5	1035	10.2	1.8	0.13
90	19.1	0.72	0.33	11.4	2.3	318	9.5	1.8	0.14
120	15.7	0.54	0.32	9.4	1.9	39	8.9	1.7	0.08
150	13.5	0.24	0.22	7.3	1.5	21	8.7	1.7	0.11
180	15.6	0.33	0.25	8.7	1.7	74	9.6	1.8	0.14
210	17.5	0.42	0.36	10.7	2.1	55	8.3	1.7	0.11
270	17.6	0.59	0.46	11.4	2.2	95	9.6	1.8	0.15
300	15.6	0.40	0.30	9.1	1.8	240	13.8	2.1	0.31
330	20.5	0.77	0.36	12.6	2.5	540	15.1	2.3	0.25

For the morphometric analysis, displacement height (z_d) and roughness length (z_0) were calculated following Bottema (1997) (his Eqs. (13) and (5), respectively). Plan (λ_p) and frontal (λ_f) area indices are also given for each wind direction sector (DIR). For the log-wind profile, non-linear least squares estimates of z_0 and z_d (m) were made from wind speed measurements at R4 and R1. N is the number of 5 min samples for each sector and RMSE is the root mean square error for the prediction of wind speed at R2 in $m\,s^{-1}$.

Fig. 3. Photos of the masts and instrumentation: roof level (left) and canyon (right).

eastward 1 m from the mast. TCs to measure air temperature are attached to each sonic in the same manner as in the canyon.

3.2. Data logging and processing

Vector wind velocities (U, V, W) and sonic temperature (T) at 10 Hz are acquired digitally and written to separate files for each sonic for each hour. The data are routinely post-processed for means and higher order statistics (variances, covariances, skewness, kurtosis) at 5 min intervals to match the output interval for the other measurements. Prior to the calculation of statistics, the data are subjected to a spike detection algorithm based on the sample deviation from a windowed mean. Wind direction is computed with respect to the canyon long axis, and vertical rotation angle (angle of attack) is computed with respect to a non-sloping plane and has not been adjusted for sonic tilt. Because the sonics are calibrated for horizontal flow, some correction of the velocities is necessary for the large angles of attack in the canyon. The angle of attack (α)-dependent vertical velocity correction of Van der Molen et al. (2004) was applied with coefficients estimated from post-field campaign data. The coefficients used for the correction function and error estimates for the wind components are given in Table 3. Horizontal velocity corrections were applied using the coefficients given in Van der Molen et al. (2004).

To investigate episodic events, statistics are calculated on much shorter intervals but using the same parameters. To enhance visual interpretation, measurements are interpolated to a finer grid in some instances. In these cases, the interpolated vectors are determined by specifying non-slip conditions at the canyon surfaces (walls, street) and replicating the above canyon measurements at measurement heights across the canyon top. The measurements and these boundary conditions
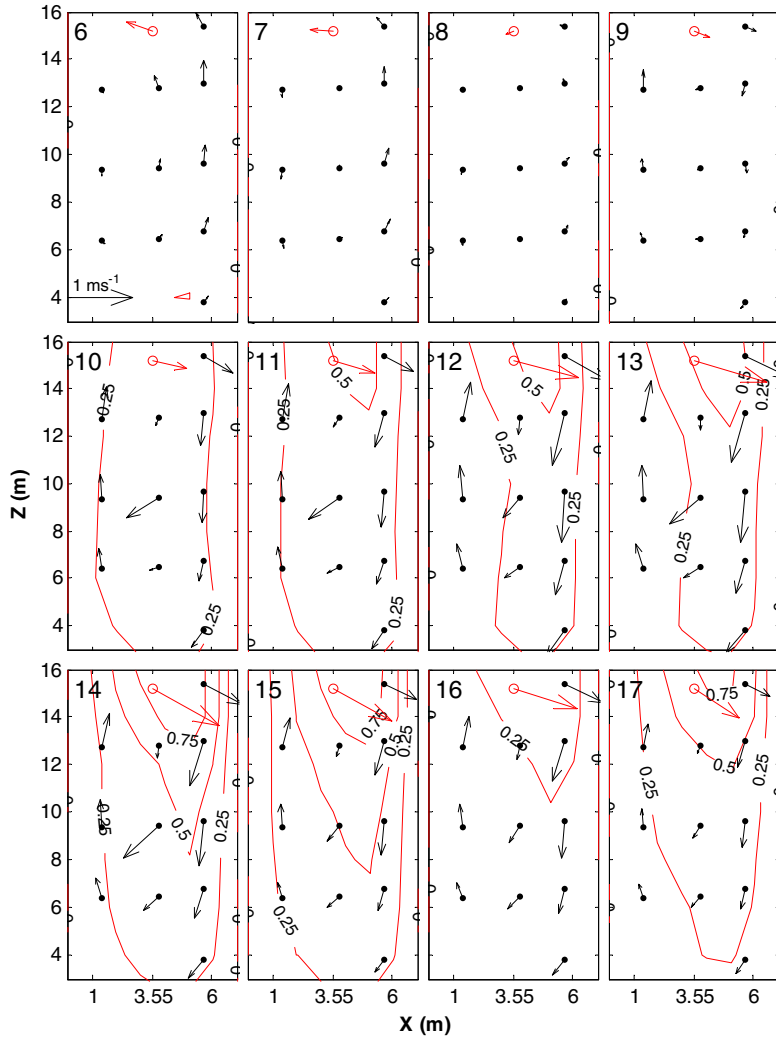
Fig. 4. Hourly averaged canyon wind fields during a land to sea breeze transition on 31 July 31 2003. Start hour is given in the upper left. Dark (black) vectors are observed fields within the canyon (*U–W* plane) scaled by a factor of 3 to the axes (a reference vector is shown in the 6 h plot). The contours show the interpolated *V* component (along canyon) of wind speed (m s^{-1}) within the canyon. The vector emanating from the circle at top centre is the reference wind (*U−V* plane) at R4 scaled directly to the axes (1 m = 1 m s^{-1}). The figure is oriented with east to the right. Note that the *Z*-axis does not extend all the way to the ground but is cut off just below the lowest sonic level (Fig. 2).

Table 3
Coefficients for angle of attack (α) dependent correction (Eqs. (1) and (2), Van der Molen et al., 2004)

	p_1 (degree^{-3})	p_2 (degree^{-2})	p_2 (degree^{-1})	p_4	Mean RE (%)
$-80 \leqslant \alpha < 0$	-9.385×10^{-7}	-3.198×10^{-5}	-3.709×10^{-3}	-2.061×10^{-2}	3.2
$0 < \alpha \leqslant 80$	-1.839×10^{-6}	9.336×10^{-5}	-2.672×10^{-3}	9.900×10^{-3}	2.9

For $|\alpha| > 80°$ the coefficients are fixed at the appropriate $\pm 80°$ values. Relative error (RE) is calculated as $c - w)/w|$, where w_c is the corrected vertical velocity and w is the accepted value.

are then interpolated to a uniformly spaced grid using the two-dimensional biharmonic spline interpolation of Sandwell (1987) as implemented in Matlab v6.5.

For the purpose of this paper we will refer to 'ambient' as pertaining to flow characteristics from the highest sonic level above the roof (R4). 'Along canyon'

refers to ambient flow parallel to the long canyon axis (*V* component) and 'across canyon' refers to ambient flow orthogonal to the long canyon axis (*U* component). Vertical flow is simply the *W* component of wind velocity. Hereafter, reference to wind direction, either cardinal or when given in degrees, is made with respect to the canyon.

3.3. Data analysed

In this paper, results and discussion concern data from 13 predominantly clear sky days during the summer and early autumn of 2003. The purpose of this restriction is to ensure that data were collected during times of no rainfall and that the primary external changes are limited to incoming solar radiation and air temperature. For the selected days, global radiation ranged from 84% to 98% of a modelled clear sky value (Bird and Hulstrom, 1991). The days used and the mean meteorological fields from the uppermost location (R4) are listed in Table 4.

4. Results and discussion

4.1. Vortex circulation under quasi steady state conditions

Under sea breeze conditions, wind direction is relatively constant, which provides one of the better opportunities to examine quasi-steady-state conditions for comparison with results from numerical and scale models. Data from a typical day (Fig. 4), 31 July 2003, show a single helical vortex pattern for the daytime sea breeze (westerly) beginning sometime after 0900 local daylight savings time (LDST) and continuing into the late afternoon hours. The flow pattern is well organised and similar throughout this period, though wind speed and direction do vary somewhat. Flow along the canyon (contours in Fig. 4) is stronger on the east side as flow is directed down into the canyon along this wall. The along canyon component also increases with respect to the turning of the ambient wind. During easterly flow (e.g. nocturnal and early morning) ambient wind speeds are low and the vortex circulation is weak but still evident (Fig. 4). These results are generally consistent with the findings of DePaul and Sheih (1986).

For canyons of this aspect ratio ($\sim$2), both numerical and scale models predict the existence of a double vortex with the separation between perhaps one-half to one-third of canyon height (e.g. Baik et al., 2000). Here, the primary circulation reaches the level of the lowest east measurement at one-quarter the canyon height ($z = 0.25$ H) when data are averaged over 5 min periods and there is no evidence of a consistent, stationary counter-rotating second vortex. However, when data are analysed over shorter time intervals and when balloons and smoke are released at ground level such patterns can be seen.

4.2. Short-term analysis

Examining the data on time intervals as short as 0.1 s, secondary vortex circulations can be found but are

Table 4
Days used for data analysis and the temperature (*T*), horizontal wind speed (WS) and direction (Dir) characteristics observed on these days at the R4 sonic (Fig. 3)

Date	Day	T_{avg} (°C)	T_{max} (°C)	T_{min} (°C)	WS (m s^{-1})	WS_{max} (m s^{-1})	WS_{min} (m s^{-1})	WS_{sd} (m s^{-1})	N	Dir_{AM}	% of time from Dir_{AM}	Dir_{PM}	% of time from Dir_{PM}
15-Jul.	196	23.5	28.3	17.4	3.0	6.0	0.6	1.2	242	NE	66.0	NE	63.2
30-Jul.	211[sb]	18.2	22.1	12.4	1.6	4.7	0.3	0.9	131	NE	41.7	NW	41.0
31-Jul.	212[sb]	19.7	23.5	14.4	1.8	4.7	0.2	0.9	138	E	35.4	SW	42.4
4-Aug.	216	18.2	19.8	17.0	3.6	6.4	1.3	1.0	286	W	79.2	NW	51.4
5-Aug.	217	19.0	21.2	16.3	1.9	4.2	0.1	0.9	183	NW	33.3	NW	54.9
6-Aug.	218[sb]	18.8	22.9	13.1	1.4	4.3	0.2	0.9	106	NE	50.7	NW	75.7
29-Sep.	272	7.1	12.3	2.0	1.8	3.5	0.9	0.6	190	E	60.4	NE	54.9
30-Sep.	273	7.0	11.8	0.9	1.7	4.0	0.5	0.8	139	E	52.8	S	43.1
11-Oct.	284	10.8	12.1	8.7	3.7	9.0	0.8	1.6	282	NW	87.5	NW	84.0
12-Oct.	285	7.4	11.0	3.5	1.6	4.9	0.0	1.2	127	N	61.1	N	56.3
13-Oct.	286	5.1	7.9	2.1	2.5	5.8	0.2	1.3	220	NE	84.7	E	55.6
14-Oct.	287	3.7	9.0	−0.3	1.6	4.2	0.3	1.0	98	NE	80.6	E	63.2
15-Oct.	288	3.1	8.5	−1.2	1.5	3.7	0.4	0.7	95	NE	72.2	E	52.8
ALL		12.4	28.3	−1.2	2.1	9.0	0.0	1.3	2237	NE	41.1	NW	25.3

N is the number of 5 min periods with $WS_{R4} > 1.5$ m s^{-1}. A sea breeze pattern is indicated by Day[sb].

infrequent and persist on the order of seconds only. As shown in Fig. 5, a weak vortex apparently develops in the lower half of the canyon counter-rotating to the upper vortex. This persists for about 10 s at which time a stronger flow penetrates down to the lower half of the canyon establishing the vortex pattern more typically seen over longer time scales (third row, Fig. 5). However, we cannot conclude that the upper vortex is

driving the lower vortex in all instances. On turbulent time scales, stacked vortices rotating in the same direction also occur. These seem to be a consequence of the penetration of stronger flow into the upper reaches of the canyon but not to the lower reaches and the lower vortex is a decaying eddy. In visualisation experiments, flow below the measurements was more frequently decoupled from the main vortex circulation
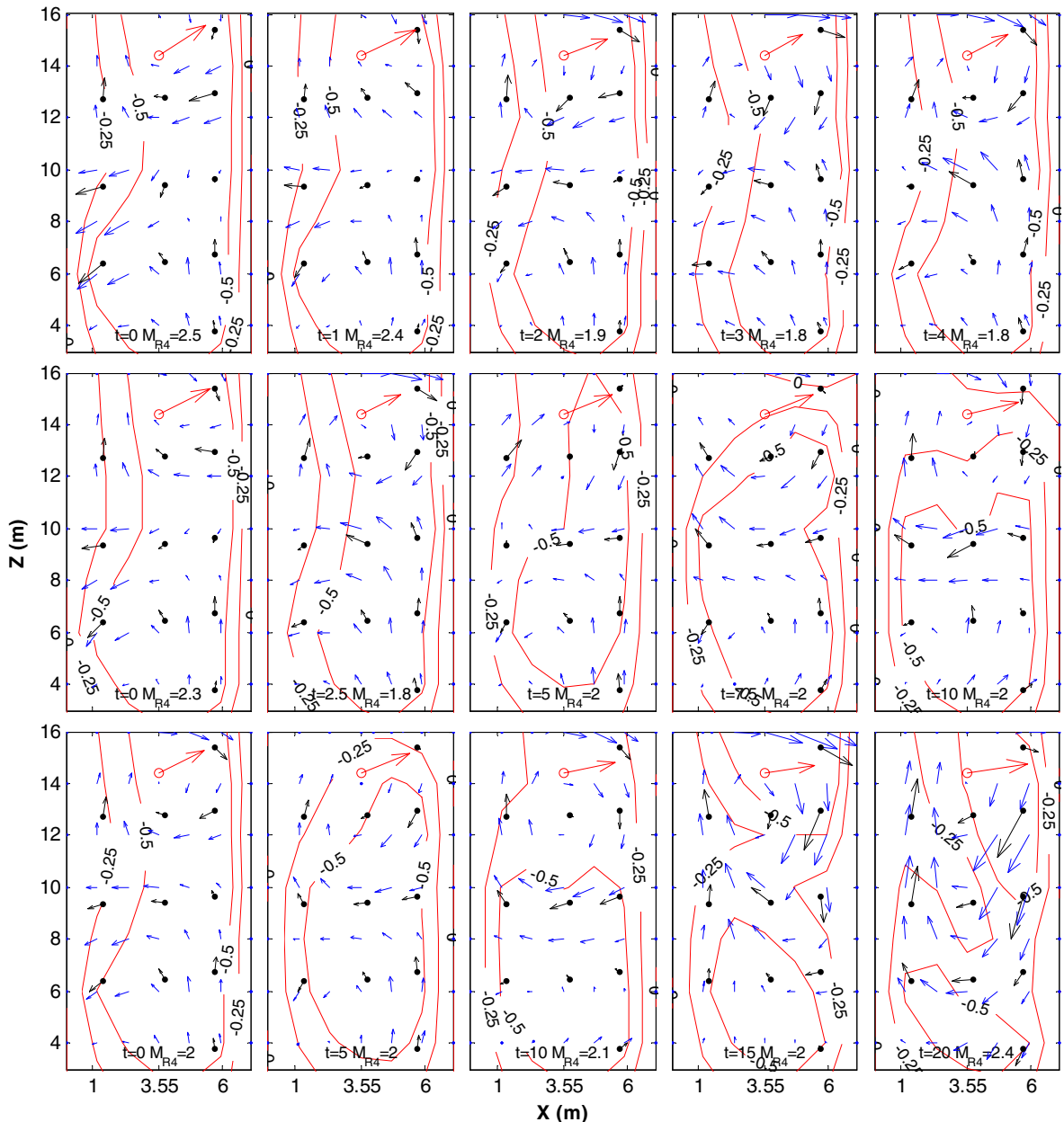
Fig. 5. Example of a secondary circulation in the lower half of the canyon. Start time (t [s]) and ambient speed (M_{R4} [m s^{-1}]) are shown for averaging periods of 1, 2.5 and 5 s for the top, middle and bottom row, respectively. Interpolated vectors are shown in grey. Other vector definitions and scaling are the same as Fig. 4.

and along canyon flow dominated. The mean vortex circulation may simply be too weak to drive a second vortex.

Short-interval 'images' of the flow field show that larger scale motions can cause rapid changes in the canyon flow field. As in Fig. 5, eddies frequently penetrate deep into the canyon essentially disrupting any established recirculation, although there is a variable lag between above and within canyon flow. This is consistent with the observations of Yamartino and Wiegand (1986) who described the vortex as rarely static in time. The strength of the circulation at these times is greater than is seen in the mean due to the turbulent nature of the flow (Louka et al., 2000). It should be noted that the surface is very rough with roughness lengths for momentum on the order of 2 m. The lack of a persistent double vortex circulation and the weakness or intermittency of the vortex circulation is in general agreement with the conclusions of Louka et al. (2000) that the mean vortex pattern should not be interpreted as a continuous phenomenon.

4.3. Flow patterns with respect to wind direction

Analysis of mean wind fields shows a consistent pattern with an elliptical helix rotated with respect to ambient wind direction. This type of circulation is evident in the mean flow field when ambient flow is more than $30°$ off parallel (Fig. 6) as suggested by Dabbert et al. (1973). However, as argued by Yamartino and Wiegand (1986), the mean flow field can show this type of circulation with ambient flow from any direction if only for a short interval of time. In the present study, this is evident since canyon flow patterns can persist through changes in ambient wind direction if wind speeds are low or turbulence weak. As seen in Fig. 7, there is a strong non-linear correlation between the wind direction at the reference level and flow throughout the canyon so long as wind speeds are sufficiently high ($> 2\,\mathrm{m\,s^{-1}}$). Wind direction is nearly linear for the above canyon levels except for flow from the northwest. Since along canyon flow dominates, winds are directed either north or south along the canyon. The exception occurs
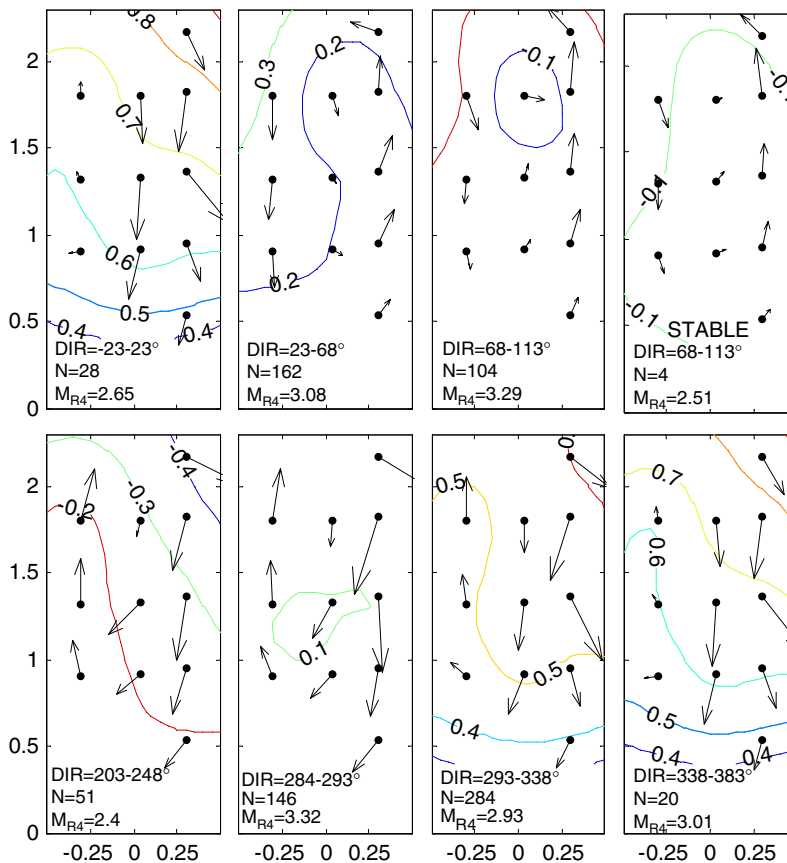
Fig. 6. Canyon wind fields in relation to above canyon wind direction (DIR, referenced to canyon orientation, see text) for all periods with ambient wind speed (M_{R4}) $> 1.5\,\mathrm{m\,s^{-1}}$. N is the number of 5 min periods (Table 4). Wind sectors with $N < 3$ are not shown. Location is normalised by width of the canyon ($W = 7.1\,\mathrm{m}$). Velocities are normalised to M_{R4} shown below each figure and are scaled by a factor of 2. Also shown is a subset of observations under stable conditions under easterly flow.
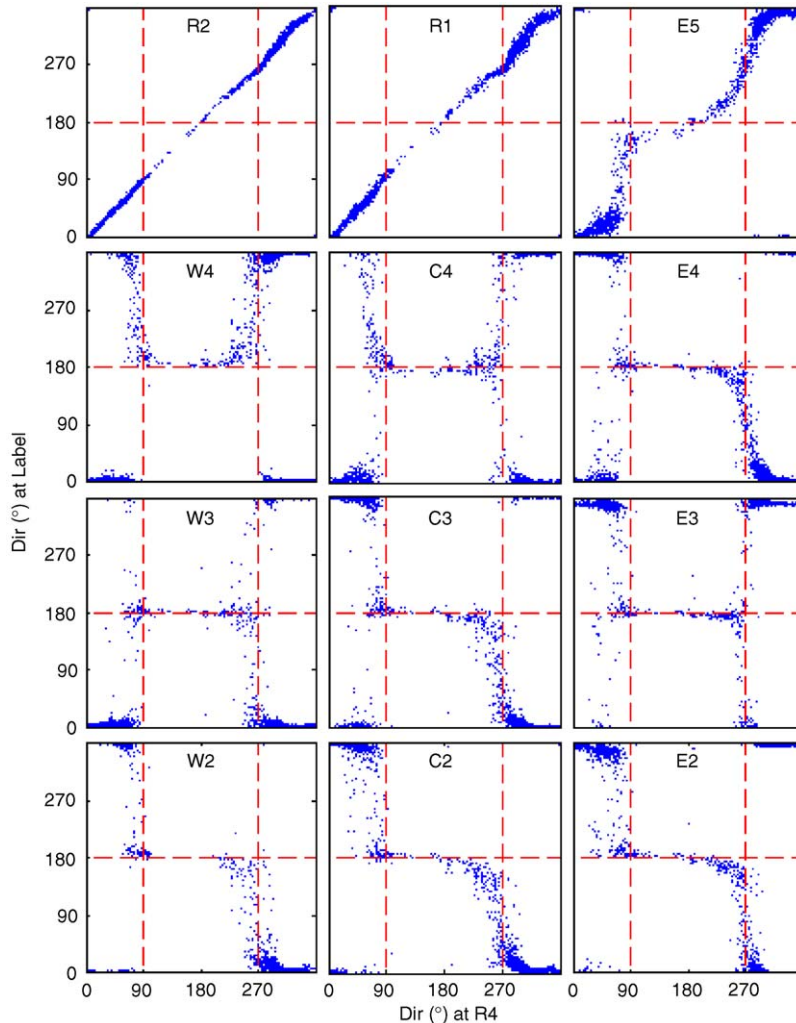
Fig. 7. Wind directions plotted against top sonic (R4) for $M_{R4} > 2\,\mathrm{m\,s}^{-1}$. Note the asymmetry for westerly and easterly flow for E5 and the reflection of flow patterns moving down into the canyon (e.g. E5 to E2).

with flow within a few degrees of perpendicular to the canyon. Here some 'reflection' of the wind vector (Nakamura and Oke, 1988; Johnson and Hunter, 1999) can be seen in the reflective symmetry in wind directions: northwesterly (southwesterly) winds become northeasterly (southeasterly) at the lower measurement levels. The uppermost level shows a somewhat different response. The W4 and C4 sonics exhibit only westerly flow for cross canyon winds. These patterns begin to break down for wind speeds less than $2\,\mathrm{m\,s}^{-1}$ and show much more scatter lower in the canyon (not shown).

Ambient flow from the west is directed more downward and into the canyon, whereas with flow from the east streamlines are directed slightly upward. For example, as shown in Fig. 7 the E5 sonic behaves more as if it were in the canyon for easterly than for westerly

flow. Thus, along canyon flow is relatively stronger with westerly flow (Fig. 6). Another consequence of this is relatively stronger vortex circulation for westerly flow and vectors nearer the east wall having greater magnitudes than those nearer the west (Fig. 6). The relative strength of the circulation in the vertical can be seen in Fig. 8. The maximum downward vertical velocity at the windward wall is twice as high for westerly compared to easterly flow (Fig. 8a).

4.4. Centre of rotation

Based solely on the measured values (Figs. 6 and 8a) the vertical centre of rotation is located between the C3 and C4 sonics (Fig. 2), in agreement with DePaul and Sheih (1986), showing a somewhat upward displacement
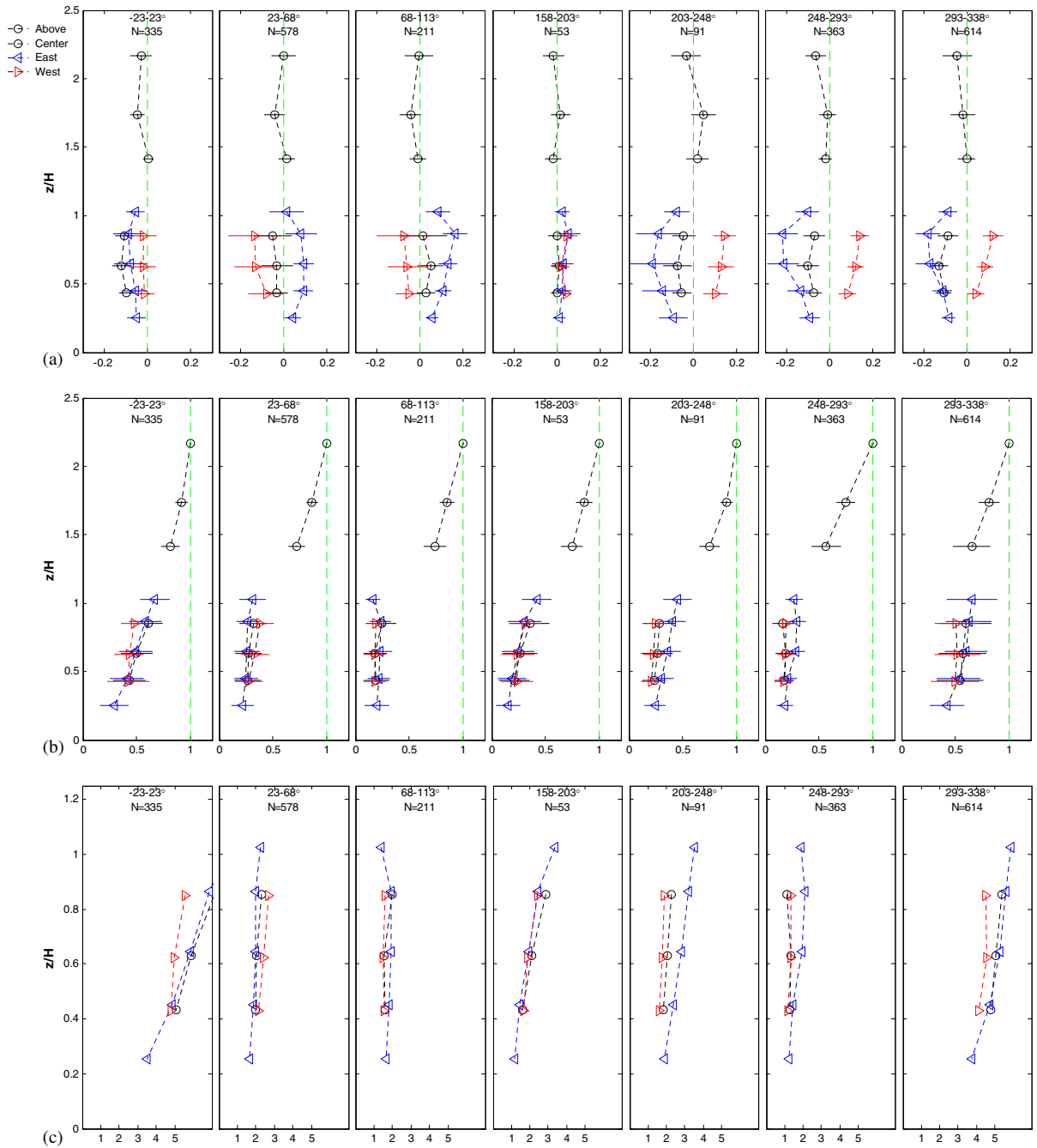
Fig. 8. Scaled velocities. Error bars are $\pm 1\sigma$. Values shown at the top of the figures are ambient wind direction and the number of 5 min observations, N. Observations restricted to $M_{R4} > 1.5\,\mathrm{m\,s^{-1}}$. *Note*: observations not available from all wind sectors. C4 and W2 have fewer observations in some instances. (a) Vertical (W/M_{R4}), (b) total speed (M/M_{R4}), (c) within canyon (M/u^*_{E5}).

with respect to the canyon centre. The downstream displacement reported by Baik et al. (2000) and Baik and Kim (2002) is not seen as the centre and east sonics follow the same patterns regardless of vortex direction. The height of this vertical centre suggests that perhaps

the effective canyon depth may be greater than that chosen here. This could be due to the aforementioned factors of roof shape and the additional rooftop obstructions. The vortex top should occur at the location of maximum shear stress, which is typically at

roof height (Louka et al., 2000). In this and other cases where roof shape is complex, it might help to define an effective roof height that could be calculated from simple geometric description.

4.5. Circulation or re-circulation?

An important question for air quality and pollution dispersion modelling is whether, or how much of the vortex circulation, is a recirculation of air within the canyon. Some mixing will occur even with a well-developed vortex as air is entrained (ejected) at the canyon top by the intermittent penetration of eddies or by downward (upward) streamlines or the mixing in the shear layer. Visual examination of the 10 Hz data show that while the larger scale eddies do not always penetrate to the lowest measurement levels, they are exchanging air at the top of the canyon. Vachon et al. (1999) calculated residence times for neutrally buoyant balloons released within a canyon of $H/W \sim 1.4$. More than 50% of the balloons had a residence time within the canyon of less than 1 min though some of these were removed via side streets. Louka et al. (2000) computes the circulation time as the time for one traverse of the perimeter based on canyon dimensions. The perimeter of this canyon box cross-section is 45 m, whereas the path of the vortex is much less. Mean vertical wind speeds within the canyon reach a maximum of $\sim 0.75\,\mathrm{m\,s^{-1}}$. Thus the circulation time is on the order of 1 min. This is much greater than the estimated 10 s for Louka et al. (2000) but it is unclear whether their mean canyon wind speed included an along canyon component. In any case the residence time is expected to be less due to along canyon flow and mixing due to end vortices.

4.6. Canyon wind velocity

Comparison between different studies is complicated by the variety of statistics (and normalisations) reported in the literature. This is exacerbated by the spatial (horizontal and vertical) variation; for example, in modelling studies the wind profile may be normalised by wind speed at roof level, a measure that is not often available in field studies and subject to marked variation in space (e.g. Rotach, 1995; Kastner-Klein et al., 2001). To avoid this complication, normalised quantities are presented with respect to the ambient flow measurements at R4 or to a local statistic, i.e. one measured at the same location. Mean total wind speed (M/M_{R4}) shows only slight differences within canyon in both the vertical profile and across the canyon for across canyon flow (Fig. 8b). Differences across the canyon are greater for westerly flow, as expected due the presumed curvature of the above canyon streamlines. The within canyon patterns are in agreement with the results presented in Kastner-Klein et al. (2001) who compared

a wind–tunnel experiment with two field experiments performed by Rotach (1995) and Louka (1998). Kastner-Klein et al. (2001) also reported a pronounced maximum at 1.25 H but this is not obvious in the present study as there were no observations at that height (Fig. 8b). Above the canyon, wind speed closely follows the log wind profile law, if one allows for the simultaneous estimation of aerodynamic roughness length (z_{0m}) and displacement height (z_d) (Table 2). These parameters estimate change most dramatically with northwesterly flow where there is a change in roughness from the river to the urban area and added relief due to the hill. The reduction in wind speed into the canyon is much less for along canyon ambient flow. This appears opposite to that measured by Rotach (1995) but similar to the findings of Christen et al. (2003).

There appears to be some divergence in wind speeds toward the canyon floor for winds orthogonal to the canyon, but at these angles the vertical velocity becomes an important component of mean flow and there is no divergence for the total wind (Fig. 8c). Louka et al. (2000) suggest that for cross-canyon flow driven by the shear stress across the top of the canyon, the recirculation in the canyon should be of the same magnitude as friction velocity at roof level. Although no measurements at the presumed height of peak shear stress was carried out in the present study, Fig. 8c shows that for cross-canyon flow the ratio of total wind speed to the friction velocity at the top canyon level has a nearly vertical profile down to the lowest measurement.

4.7. Turbulence statistics

4.7.1. Vertical velocity fluctuations

To model dispersion of air pollutants and the exchange of energy, it is important to know how turbulence varies within the canyon. Commonly cited is the ratio of the standard deviation of vertical velocity to local friction velocity (σ_w/u^*, Fig. 9a). Within the inertial sublayer under neutral stability, σ_w/u^* should be approximately 1.25 (Roth, 2000). Fig. 9a shows that vertical mixing is greatly enhanced within the canyon relative to the local friction velocity with values reaching $\sigma_w/u^* = 2$ but declines rapidly near the canyon top, and may be diminished in some cases, owing to the strong shear layer. Similar magnitudes and patterns are shown by Rotach (1995) and Christen et al. (2003).

A simplified picture within the canyon may be obtained by scaling σ_w by the top-level wind speed (Fig. 9b). For cross-canyon flow, the windward wall has heightened mixing in the vertical relative to the rest of the canyon. The values across the canyon tend to converge at the canyon top and lowest measurement level. For along canyon winds, a single profile exists (Fig. 9b). The peak of σ_w in relative, and absolute, terms
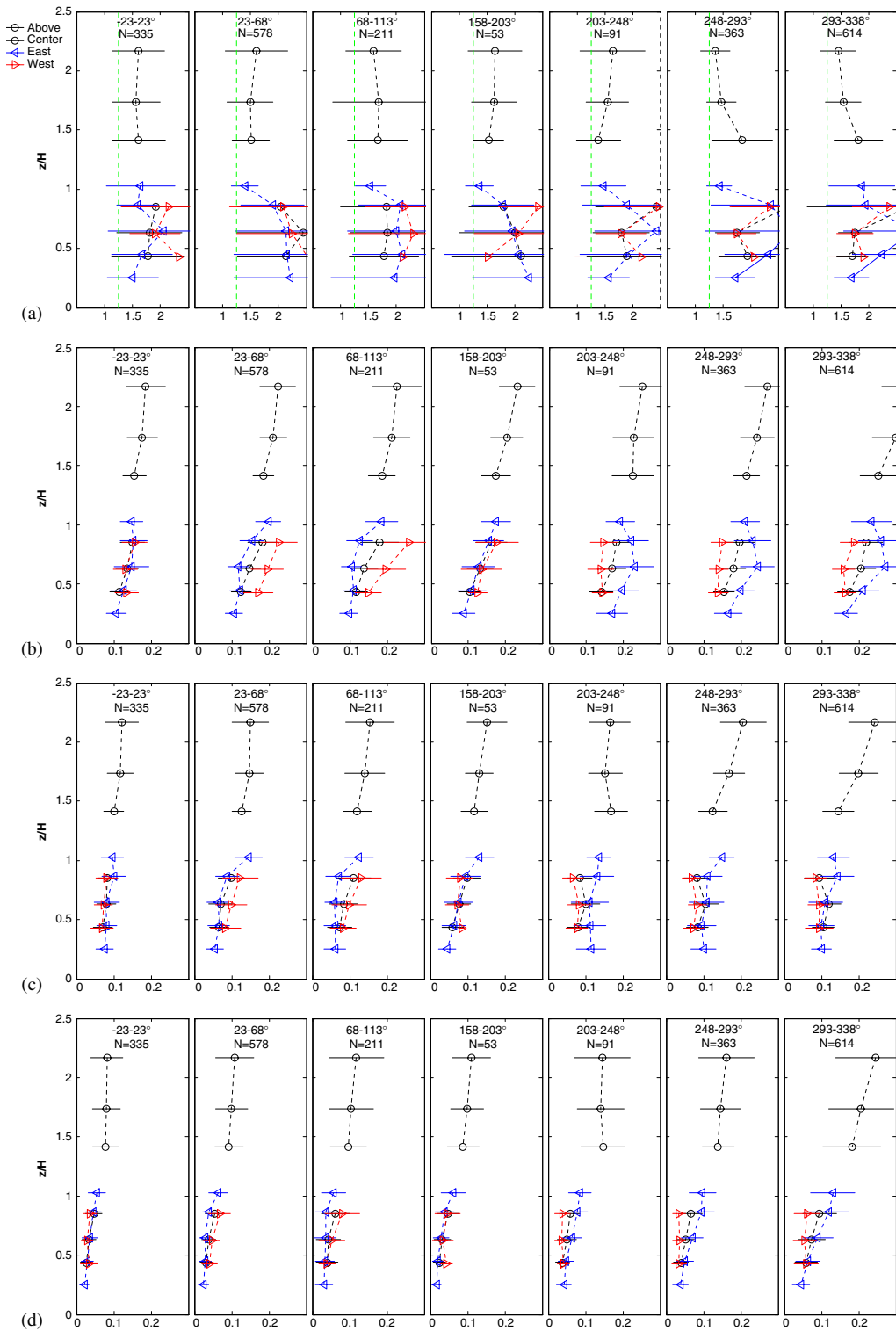
Fig. 9. Normalized turbulence statistics: (a) vertical standard deviation (σ_w/u^*) with a vertical reference at $\sigma_w/u^* = 1.25$. (b) σ_w/M_{R4} (c) u^*/M_{R4}. (d) TKE/M_{R4}^2.

varies with ambient flow. It peaks within the canyon for westerly flow and above the canyon for easterly flow.

4.7.2. Friction velocity

Numerical and scale models predict a strong shear layer at the roof top level. This has also been identified in field experiments. However, the choice of normalisation makes comparison difficult. Data from the present study shows that the peak relative horizontal stress occurs above the canyon top for easterly flow and within the canyon for westerly flow, similar to the noted peaks in σ_w (Fig. 9b). Scaling u^* by M_{R4} shows that above the canyon there is only a slight gradient from R2 to R4, except from the northwest where a difference is expected due to local topography (Fig. 9c). Louka et al. (2000) report that the maximum Reynold's stress was found close to building tops and were 2–5 times higher than values at highest measurement level, $z = 2.26\,H$, which was considered to be above the roughness sublayer (RSL). Christen et al. (2002) observed peaks in turbulent shear stress just above roof-level. Kastner-Klein and Rotach (2004) found peaks in the shear stress between H and 1.5 H while peak values of Reynold's stress or friction velocity were observed at between 1.5 and 2 H by Rotach (1993a, b, 1995) and Oikawa and Meng (1995). Above the RSL (above at least 2 H), Reynold's stress has been observed to be relatively constant with height (Feigenwinter et al. 1999). In the present sudy u^*/M_{R4} increases with height near the canyon top (Fig. 9c) for cross-canyon flow, and may peak between H and 1.5 H for easterly flow, however, the measurement locations limit the interpretability. For northwesterly flow u^*/M_{R4} continues to increase with height above the canyon so that such a peak is unlikely.

4.7.3. Turbulence kinetic energy (TKE)

The profiles of turbulent kinetic energy (Fig. 9d) show a pattern similar to the other turbulence statistics presented in Fig. 9. Within the canyon, particularly nearest the leeward wall, the profile is nearly vertical with height. Also, the profiles predictably converge toward the canyon bottom. At the canyon centre and nearer the downstream or windward wall, TKE increases with height. These are nearly identical results to those obtained by Brown et al. (2000) and Baik and Kim (2002) within scale model canyons. In Brown et al. (2000) within canyon profiles shows nearly uniform TKE up to 0.8 H where TKE starts to increase, reaching a peak at about 1.5 H. In Fig. 9d profiles are uniform up to about 0.7 H with an increasing TKE up to R1 (1.5 H) and thereafter a nearly vertical profile up to R4 (2.2 H). Another interesting result from Brown et al. (2000) is that the profile at the downstream side of each canyon showed nearly twice the TKE as compared to the other in-canyon profiles. This is not evident from the data presented in Fig. 9d.

5. Conclusions

The results show a clear pattern of vortex development and circulation, driven by a shear layer at the effective roof height. Even under the best scenario of a near stationary flow regime (summertime sea breeze) the flow within the canyon may change rapidly due to the penetration of the shear layer. A combination of complex building roof shapes and local topography may contribute to this effect by maintaining a high degree of turbulence even under low wind speed conditions. In addition, the intermittency may help maintain the mean circulation that appears to penetrate to the lowest measurement level. Despite this complexity, a vortex is shown to form for wind directions within 60° perpendicular to the canyon long axis as qualitatively observed in earlier studies.

A secondary vortex circulation exists for short time periods (order of seconds) in the lower portion of the canyon during conditions with low wind speeds and weak turbulence. Results show both secondary vortices that are counter rotating and ones that rotate in the same direction as the upper vortex. Visualisation experiments show that flow below the lowest measurements was more frequently decoupled from the main vortex circulation and along canyon flow dominated. Further analysis is, however, needed to determine whether such patterns are driven by the upper vortex, or are the result of a prior circulation displaced in space. Restrictions on measurements close to street level limit the observation of probable persistent secondary circulations below 0.4 H, however, these are being investigated on a short-term case study basis.

While mean and turbulence statistics generally seem to be in agreement with other canyon studies, direct comparison is difficult. In this study, the results indicate a high degree of vertical mixing within the canyon. Total wind speed, friction velocity and TKE are nearly constant with height from 0.25 to 0.5 H for cross-canyon flow. Across the canyon, mixing and turbulence are greater nearer the windward wall but converge to uniform values as the measurement height decreases. For along-canyon flow, turbulence statistics are close to equal over most of the canyon (0.2 to 0.8W) for along canyon flow.

References

Allwine, K.J., Shinn, J.H., Streit, G.E., Clawson, K.L., Brown, M., 2002. Overview of URBAN 2000: a multiscale field study of dispersion through an urban environment. qBulletin of the American Meteorological Society 83, 521–536.

Arnfield, A.J., 1982. An approach to the estimation of the surface radiative properties and radiation budgets of cities. Physical Geography 3, 97–122.

Arnfield, A.J., Mills, G.M., 1994. An analysis of the circulation characteristics and energy budget. I. Circulation characteristics. International Journal of Climatology 14, 119–134.

Baik, J.-J., Kim, J.-J., 1999. A numerical study of flow and pollutant dispersion characteristics in urban street canyons. Journal of Applied Meteorology 38 (11), 1576–1589.

Baik, J.-J., Kim, J.-J., 2002. On the escape of pollutants from urban street canyons. Atmospheric Environment 36, 527–536.

Baik, J.-J., Park, R.-S., Chun, H-Y., Kim, J-J., 2000. A laboratory model of urban street–canyon flows. Journal of Applied Meteorology 39, 1592–1600.

Bird, R.E., Hulstrom, R.L., 1991. A simplified clear sky model for direct and diffuse insolation on horizontal surfaces. SERI Technical Report SERI/TR-642-761, February 1991. Solar Energy Research Institute, Golden, CO.

Brown, M.J., Lawson, R.E., Decroix, D.S., Lee, R.L., 2000. Mean flow and turbulence measurements around a 2-D array of buildings in a wind tunnel. LA-UR-99-5395, Los Alamos National Laboratory, Los Alamos, New Mexico 87545. 11th Joint AMS/AWMA Conference on the Application of Air Pollution Meteorology, Long Beach, CA, January 2000.

Brown, M.J., Boswell, D., Streit, G., Nelson, M., McPherson, T., Hilton, T., Pardyjak, E.R., Pol, S., Ramamurthy, P., Hansen, B., Kastner-Klein, P., Clark, J., Moore, A., Walker, D., Felton, N., Strickland, D., Brook, D., Princevac, M., Zajic, D., Wayson, R., MacDonald, J., Fleming, G., Storwold, D., 2004. Joint urban 2003 street canyon experiment. 2004 AMS Annual Meeting Symposium on Planning, Nowcasting, and Forecasting in the Urban Zone Seattle WA, January 2004.J7.3.

Christen, A., Vogt, R., Rotach, M.W., Parlow, E., 2002. First results from Bubble, Partitioning of turbulent heat fluxes and urban surfaces. AMS Conference on the Urban Environment, pp. 105–106.

Christen, A., Vogt, R., Rotach, M.W., 2003. Profile measurements of selected turbulence parameters over different urban surfaces. Fourth International Conference on Urban Air Quality, Prague, 25–27 March 2003, pp. 408–411.

Dabbert, W.F., Ludwig, F.L., Johnson Jr., W.B., 1973. Validation and applications of an urban diffusion model for vehicular pollutants. Atmospheric Environment 7, 603–618.

Davidson, M.J., Mylne, K.R., Jones, C.D., Phillips, J.C., Perkins, R.J., Fung, J.C.H., Hunt, J.C.R., 1995. Plume dispersion through large groups of obstacles—a field investigation. Atmospheric Environment 29, 3245–3256.

DePaul, F.T., Sheih, C.M., 1986. Measurements of wind velocities in a street canyon. Atmospheric Environment 20, 45–459.

Feigenwinter, C., Vogt, R., Parlow, E., 1999. Vertical structure of selected turbulence characteristics above an urban canopy. Theoretical and Applied Climatology 62, 51–63.

Grimmond, C.S.B., Potter, S.K., Zutter, H.N., Souch, C., 2001. Rapid methods to estimate sky-view factors applied to urban areas. International Journal of Climatology 21, 903–913.

Johnson, G.T., Hunter, L.J., 1999. Some insights into typical urban canyon airflows. Atmospheric Environment 33, 3991–3999.

Johnson, W.B., Ludwig, F.L., Dabberdt, W.F., Allen, R.J., 1973. An urban diffusion simulation model for carbon monoxide. Journal of Air Pollution Control Association, 490–498.

Kastner-Klein, P., Rotach, M., 2004. Mean flow and turbulence characteristics in an urban roughness sublayer. Boundary-Layer Meteorology 111, 55–84.

Kastner-Klein, P., Fedorovich, E., Rotach, M.W., 2001. A wind tunnel study of organised and turbulent air motions in urban street canyons. Journal of Wind Engineering and Industrial Aerodynamics 89, 849–861.

Kim, J-J., Baik, J-J., 2001. Urban street–canyon flows with bottom heating. Atmospheric Environment 35, 3395–3404.

Kovar-Panskus, A., Louka, P., Sini, J.-F., Savory, E., Czech, M., Abdelqari, A., Mestayer, P.G., Toy, N., 2002. Influence of geometry on the mean flow within urban street canyons—a comparison of wind tunnel experiments and numerical simulations. Water, Air, and Soil Pollution: Focus 2, 365–380.

Louka, P., 1998. Measurements of air flow in an urban environment. Ph.D. Thesis, University of Reading.

Louka, P., Belcher, S.E., Harrison, R.G., 2000. Coupling between air flow in streets and the well-developed boundary layer aloft. Atmospheric Environment 34, 2613–2621.

Louka, P., Vachon, G., Sini, J.-F., Mestayer, P.G., Rosant, J.-M., 2002. Thermal effects on the airflow in a street canyon—Nantes'99 experimental results and model simulations. Water, Soil and Air Pollution: Focus 2, 351–364.

Nakamura, Y., Oke, T.R., 1998. Wind, temperature and stability conditions in an east–west oriented urban canyon. Atmospheric Environment 22, 2691–2700.

Nielsen, M., 2000. Turbulent ventilation of a street canyon. Environmental Monitoring and Assessment 65, 396–398.

Oikawa, S., Meng, Y., 1995. Turbulence characteristics and organized motion in a suburban roughness sublayer. Boundary-Layer Meteorology 74, 289–312.

Oke, T.R., 1988. Street design and urban canopy layer climate. Energy and Buildings 11, 103–113.

Rafailidis, S., 1997. Influence of building areal density and roof shape on the wind characteristics above a town. Boundary-Layer Meteorology 85, 255–271.

Rotach, M.W., 1993a. Turbulence close to a rough urban surface.1. Reynolds stress. Boundary-Layer Meteorology 65, 1–28.

Rotach, M.W., 1993b. Turbulence close to a rough urban surface 2. Variances and gradients. Boundary-Layer Meteorology 66, 75–92.

Rotach, M.W., 1995. Profiles of turbulence statistics in and above an urban street canyon. Atmospheric Environment 29, 1473–1486.

Roth, M., 2000. Review of atmospheric turbulence over cities. Quarterly Journal of the Royal Meteorological Society 126, 941–990.

Sandwell, D.T., 1987. Biharmonic spline interpolation of GEOS-3 and SEASAT altimeter data. Geophysical Research Letters 2, 139–142.

Santamouris, M., Papanikolaou, Koronakis, I., Livada, I., Asimakopoulos, D., 1999. Thermal and air flow characteristics in a deep pedestrian canyon under hot weather conditions. Atmospheric Environment 33, 4503–4521.

Sini, J., Anquetin, S., Mestayer, P., 1996. Pollutant dispersion and thermal effects in urban street canyons. Atmospheric Environment 30, 2659–2677.

Vachon, G., Rosant, J.-M., Mestayer, P., Sini, J.-F., 1999. Measurements of dynamic and thermal field in a street canyon. URBCAP Nantes 99. Proceedings of the Sixth International Conference on Harmonisation within Atmo-

spheric Dispersion Modelling, 11–14 October, Rouen, France, 12pp.

Van der Molen, M.K., Gash, J.H.C., Elbers, J.A., 2004. Sonic anemometer (co)sine response and flux measurement II. The effect of introducing an angle of attack dependent calibration. Agricultural and Forest Meteorology 122, 95–109.

Vardoulakis, S., Fisher, B.E.A., Pericleous, K., Gonzalez-Flesca, N., 2003. Modelling air quality in street canyons: a review. Atmospheric Environment 37, 155–182.

Yamartino, R.J., Wiegand, G., 1986. Development and evaluation of simple models for the flow, turbulence, and pollutant concentration fields within an urban street canyon. Atmospheric Environment 20, 2137–2156.

Zajic, D., Fernando, H.J.S., Brown, M.J., Kim, J.-J., Baik, J.-J., 2003. Flow and turbulence in simulated city canyons: measurements and computations. Fifth International Conference on Urban Climate, Łodz, Poland, 1–5 September 2003, O.33.4.